Neuron, Vol. 46, 787–798, June 2, 2005, Copyright ©2005 by Elsevier Inc. DOI 10.1016/j.neuron.2005.04.035

Behavioral Correlates of Activity in Identified Hypocretin/Orexin Neurons

Boris Y. Mileykovskiy,[1,3,4,*] Lyudmila I. Kiyashchenko,[1,3,4] and Jerome M. Siegel[1,2,3,*]

[1]Department of Psychiatry and Biobehavioral Sciences
[2]Brain Research Institute
University of California, Los Angeles
Los Angeles, California 90095
[3]Veterans Administration Greater Los Angeles Healthcare System-Sepulveda
North Hills, California 91343

Summary

Micropipette recording with juxtacellular Neurobiotin ejection, linked micropipette-microwire recording, and antidromic and orthodromic activation from the ventral tegmental area and locus coeruleus were used to identify hypocretin (Hcrt) cells in anesthetized rats and develop criteria for identification of these cells in unanesthetized, unrestrained animals. We found that Hcrt cells have broad action potentials with elongated later positive deflections that distinguish them from adjacent antidromically identified cells. They are relatively inactive in quiet waking but are transiently activated during sensory stimulation. Hcrt cells are silent in slow wave sleep and tonic periods of REM sleep, with occasional burst discharge in phasic REM. Hcrt cells discharge in active waking and have moderate and approximately equal levels of activity during grooming and eating and maximal activity during exploratory behavior. Our findings suggest that these cells are activated during emotional and sensorimotor conditions similar to those that trigger cataplexy in narcoleptic animals.

Introduction

Hypocretin (Hcrt or orexin) was discovered in 1998 (de Lecea et al., 1998; Sakurai et al., 1998). Anatomical studies showed that neurons synthesizing this peptide project to brain monoaminergic cell groups, including cells containing norepinephrine, serotonin, histamine, and dopamine (Peyron et al., 1998). Hcrt cells also project strongly to cholinergic cells in the basal forebrain and brainstem and to other brain regions (Nambu et al., 1999; Peyron et al., 1998). Hcrt has been found to be excitatory to target neurons (Bayer et al., 2001; Brown et al., 2001; Burlet et al., 2002; Eggermann et al., 2001; Horvath et al., 1999; Korotkova et al., 2003; Li et al., 2002; Soffin et al., 2002). Hcrt cells receive projections from the medial and ventrolateral preoptic area, medial bed nucleus of the stria terminalis, lateral septum, posterior hypothalamus, ventral tegmental area (VTA), locus coeruleus (LC), and dorsal raphe (Yoshida et al., 2004).

Hcrt null mutant mice exhibit symptoms of narcolepsy including periodic losses of muscle tone during certain behaviors, and disrupted sleep and waking states (Chemelli et al., 1999). Genetically narcoleptic dogs have mutations of Hcrt receptor-2 (Lin et al., 1999). Human narcolepsy is linked to a relatively selective loss of Hcrt cells (Peyron et al., 2000; Thannickal et al., 2000; Thannickal et al., 2003), whereas Hcrt levels are normal in most other neurodegenerative disorders (Ripley et al., 2001).

The link between Hcrt cell loss and narcolepsy led to investigations of how the activity of these cells might be modulated across the sleep-wakefulness (S-W) cycle. An indirect way to address this question is by monitoring c-Fos expression. Estabrooke et al. (2001) reported that c-Fos immunoreactivity in Hcrt cells in rats was elevated in waking and was reduced during periods containing both slow wave (SW) and rapid eye movement (REM) sleep, suggesting that Hcrt cellular activity was minimal at these times. In contrast, a study in freely moving cats showed that Hcrt release in the hypothalamus and basal forebrain was increased in REM sleep (Kiyashchenko et al., 2002). Thus, direct recording of the neuronal activity of Hcrt cells is required to determine the nature of their sleep cycle discharge.

Many studies, some conducted long before the discovery of Hcrt/orexin, have investigated S-W cycle discharge in cells in the Hcrt-containing regions of the hypothalamus (Beyer et al., 1971; Findlay and Hayward, 1969; Glotzbach et al., 1987; Izumi, 1968; Parmeggiani et al., 1987; Steininger et al., 1999; Vanni-Mercier et al., 1984). Most studies reported that cells in this region were active in wakefulness and had diminished activity in SW sleep. Both increased unit activity and decreased unit activity were seen in REM sleep. Recent studies, in general, confirmed these results. About 30%–50% of perifornical (PFH) and lateral hypothalamic (LH) neurons have maximal activity in both active waking (AW) and REM sleep. About 20%–40% of neurons are most active in wakefulness, and only about 8% of neurons are most active in SW sleep (Alam et al., 2002; Koyama et al., 2003). Prior studies did not identify Hcrt cells. Furthermore, none characterized the waking behavioral correlates of discharge in hypothalamic cell types.

The VTA receives dense Hcrt projections and is a major region of passage of Hcrt axons to the caudal brainstem and spinal regions (Peyron et al., 1998; Nambu et al., 1999). Twenty percent of cells in the PFH and LH that project to the VTA contain Hcrt (Fadel and Deutch, 2002). Therefore, VTA stimulation would be likely to antidromically activate a large percentage of Hcrt cells. Recent studies (Espana et al., 2005) have shown that approximately 10% of Hcrt neurons send ipsilateral projections to the LC. Thus, the LC also would be an area from which Hcrt cells could be antidromically driven.

In the present paper, we use juxtacellular labeling to demonstrate the possibility of identification of Hcrt

*Correspondence: bmileyko@ucla.edu (B.Y.M.); jsiegel@ucla.edu (J.M.S.)
[4]These authors contributed equally to this work.

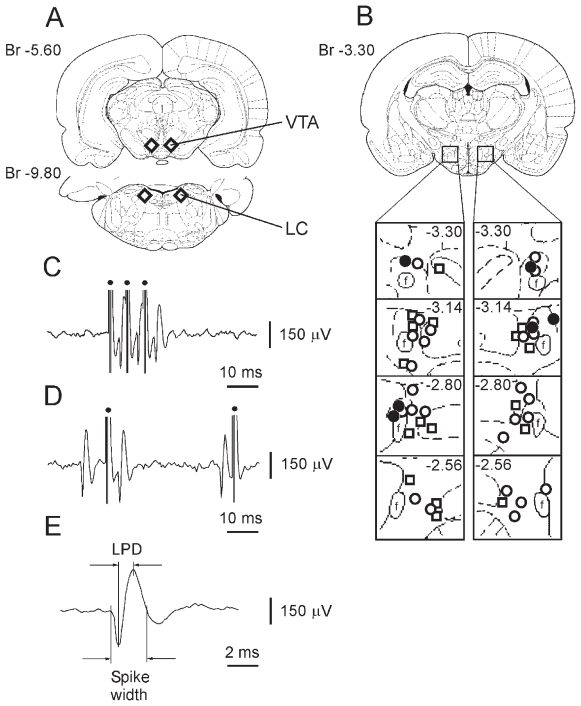

Figure 1. The Location of Stimulated VTA and LC Sites and Characteristics of Antidromically and Orthodromically Identified Hcrt Neurons Recorded in Urethane-Anesthetized Rats

(A) Schematic drawing of stimulated VTA and LC regions (diamonds) that induced antidromic and orthodromic responses in Hcrt neurons.

(B) The location of Hcrt neurons that responded antidromically (open circles) and orthodromically (open squares) to VTA stimulation as well as Hcrt cells antidromically driven by LC stimulation (closed circles).

(C) Antidromic spikes of Hcrt neuron to electrical train stimulation of the VTA.

(D) Collision of orthodromic and antidromic spikes in axon of an Hcrt neuron.

(E) Spike of Hcrt neuron recorded with micropipette. f, fornix. Dots, stimulating pulses.

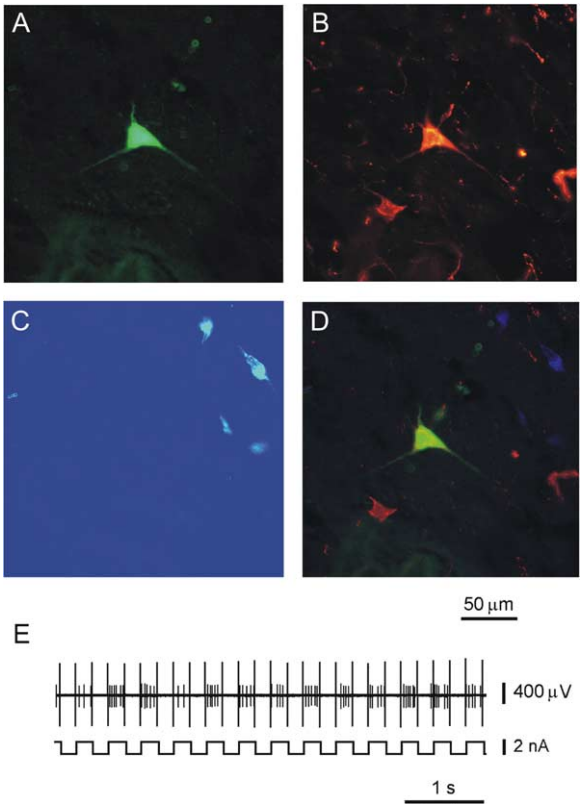

Figure 2. Immunohistochemical Identification of an Hcrt Neuron that Responded Antidromically to VTA Electrical Stimulation

(A) Neuron labeled juxtacellularly for 5 min with 4% Nb dissolved in 0.5 M CH_3COOK.

(B) This neuron expresses immunoreactivity for Hcrt.

(C) This neuron does not show immunoreactivity for MCH.

(D) Merged composite of (A) and (B).

(E) Juxtacellular labeling of Hcrt neuron with current pulses of two nA (200 ms on/200 ms off).

cells in unrestrained, behaving animals with antidromic VTA and LC electrical stimulation combined with action potential waveform analysis. We then document the discharge patterns of Hcrt neurons across the S-W cycle and during waking behaviors.

Results

Identification of Hcrt Neurons in Anesthetized Rats

VTA Electrical Stimulation

A total of 202 PFH and LH neurons were antidromically identified during electrical stimulation of the ipsilateral VTA (Figure 1A). Sixty of the antidromically identified cells were juxtacellularly labeled with Neurobiotin (Nb). Subsequent immunostaining revealed that 26 Nb-labeled cells stained for Hcrt (Figure 2). These Hcrt+/Nb+ cells had long-duration spikes with a long-lasting later positive deflection (LPD), responded antidromically with short latency to stimulation, and were located predominantly in the PFH and the medial part of the LH (Figures 1B–1E; Table 1). Most Hcrt neurons had spontaneous activity and discharged with a slow firing rate under urethane anesthesia (Table 1). The duration of the LPD for spontaneous spikes from Hcrt neurons ranged from 0.83 ms to 1.1 ms with a mean of 0.93 ± 0.02 ms (n = 22) and did not significantly differ from the LPD of spikes elicited antidromically (Table 1) in these cells ($t = 1.45$; $p = 0.16$).

The second group of antidromically identified and juxtacellularly labeled cells within the Hcrt cell field (n = 34) did not show immunoreactivity to either Hcrt or melanin-concentrating hormone (MCH). They had spikes with LPDs (Table 1) that were shorter than the LPDs of Hcrt neurons ($t = 12.3$; $p < 0.0001$). The majority of cells in this group did not have spontaneous activity in the anesthetized rat and responded antidromically with a wide range of latencies.

Electrical stimulation of the ipsilateral VTA also evoked orthodromic responses with latencies between 2 and 18 ms in 107 PFH and LH neurons. Thirty-two of them had spike LPDs ranging from 0.9 ms to 1.33 ms. Successful juxtacellular labeling of 24 neurons in this group revealed that 17 cells exhibited immunoreactivity to

Table 1. Electrophysiological Characteristics of PFH and LH Neurons Recorded with Micropipette in Urethane-Anesthetized Rats

Cell Type	Total Number	Number of Spontaneously Active Cells	Type of Response	Latency	Spike Duration	Spike LPD	Spontaneous Firing Rate
Hcrt	26	22	antidromic	5.55 ± 0.48 min = 2.02 max = 11.03	2.44 ± 0.04 min = 2.00 max = 2.81	0.90 ± 0.01 min = 0.82 max = 1.03	2.4 ± 0.4 min = 0.3 max = 6.5
Non-Hcrt/ non-MCH	34	8	antidromic	6.10 ± 0.69 min = 1.41 max = 17.12	1.85 ± 0.04 min = 1.40 max = 2.31	0.69 ± 0.01 min = 0.51 max = 0.79	7.3 ± 2.9 min = 1.8 max = 24.2
Hcrt	17	13	orthodromic	2.8–12.0	2.84 ± 0.08 min = 2.20 max = 3.71	1.03 ± 0.02 min = 0.90 max = 1.17	2.5 ± 0.3 min = 0.2 max = 4.7
Non-Hcrt/ non-MCH	7	6	orthodromic	3.0–10.5	2.64 ± 0.16 min = 2.02 max = 3.12	0.99 ± 0.06 min = 0.80 max = 1.21	3.3 ± 0.6 min = 1.6 max = 5.2

The latency, spike duration, spike LPD (ms), and spontaneous firing rate (Hz) are mean ± SEM.

Hcrt and were also located in the PFH and the medial part of the LH (Figure 1B). These Hcrt cells had an average spike LPD (Table 1) that was significantly broader than the average LPD for spontaneous spikes recorded from antidromically identified Hcrt (n = 22) and non-Hcrt (n = 8) neurons (t = 6.07; t = 14.07; $p < 0.0001$). Thirteen Hcrt cells in this group discharged spontaneously under urethane anesthesia (Table 1) and increased their firing rate up to 6.3 ± 0.4 spikes/s (min = 4.3 spikes/s; max = 9.1 spikes/s; n = 13) during VTA stimulation (3 Hz; 300–550 μA; 0.2 ms). The remaining seven cells (Table 1) did not stain for either Hcrt or MCH.

Thus, our results demonstrate that all Hcrt cells (n = 26) antidromically identified by VTA stimulation have long-duration spikes with an LPD > 0.82 ms and are located in the PFH and the medial part of the LH. Therefore, the probability of recording non-Hcrt cells meeting these criteria is <1/26 ($p < 0.04$). On the other hand, orthodromic spikes with an LPD > 0.82 ms recorded in PFH and LH neurons during VTA stimulation indicate probable Hcrt neurons but do not guarantee identification of these cells in anesthetized rats, as only 17/24 of such cells were Hcrt neurons.

LC Electrical Stimulation

A total of 104 PFH and LH neurons were antidromically identified during electrical stimulation of the ipsilateral LC (Figure 1A). Nb labeling and subsequent immunostaining revealed that six cells of these cells were Hcrt positive. All six of these neurons discharged with long-duration spikes (2.47 ± 0.12 ms; min = 2.2 ms; max = 2.9 ms; n = 6) that had long-lasting LPDs that ranged from 0.82 ms to 0.96 ms with a mean of 0.89 ± 0.02 ms (n = 6). The average LPD for this Hcrt cell group did not significantly differ from the average LPD of Hcrt neurons antidromically identified by VTA stimulation (t = 0.19; $p = 0.85$). These Hcrt neurons responded antidromically to LC stimulation with latencies that ranged from 6.2 ms to 13.1 ms with a mean of 9.23 ± 1.25 ms (n = 6) and were located predominantly in the PFH and lateral hypothalamus (Figure 1B).

Twenty-six PFH and LH neurons that had shorter-spike LPDs that ranged from 0.59 ms to 0.76 ms with a mean of 0.66 ± 0.01 ms (n = 26) were labeled with Nb. None of them showed immunoreactivity to either Hcrt or MCH. Like neurons identified by VTA stimulation, Hcrt and non-Hcrt neurons responding antidromically to LC stimulation had significantly different average LPDs (t = 9.74; $p < 0.0001$). Thus, broad spikes with an LPD > 0.82 ms would serve as criterion for identification of Hcrt neurons during LC stimulation. However, the probability of encountering Hcrt neurons with LC stimulation is low (6/104) compared to that with VTA stimulation (26/202). We also found that LC stimulation produced a pronounced movement artifact that frequently displaced the recording micropipette or microwire from the recorded cell, whereas VTA stimulation did not have this effect. Therefore, we chose VTA stimulation for identification of Hcrt cells in combined micropipette/microwire recording in anesthetized rats and in behavioral experiments.

Comparisons of Micropipette and Microwire Recording

Micropipettes do not allow stable unit recording in unrestrained animals. However, such recording can be achieved with microwires. To apply the LPD criterion obtained above for unit recording with microwires, we estimated the influence of three factors on the LPD value: (1) the decrease of input impedance during microwire recording, (2) the decrease of spike amplitude during microwire recording, and (3) the possible influence of urethane anesthesia. For this purpose, antidromic spikes of 13 Hcrt neurons (LPD > 0.82 ms) were recorded simultaneously with composite electrodes that consisted of a glass micropipette to which a 12.5 μm diameter microwire was attached. The amplitude of spikes recorded with the micropipette ranged from 136 μV to 470 μV with a mean of 277 ± 29 μV (n = 13). The same spikes recorded with the attached microwire had an amplitude that ranged from 59 μV to 100 μV with a mean of 77 ± 3 μV (n = 13). The LPDs for spikes recorded with micropipette and microwire ranged from 0.82 ms to 1.2 ms with a mean of 0.95 ± 0.02 ms (n = 13) and from 0.56 ms to 0.7 ms with a mean of 0.62 ± 0.01 ms (n = 13), respectively. The difference of LPDs recorded simultaneously with micropipette and microwire (ΔLPD) was proportional to the ratio between the

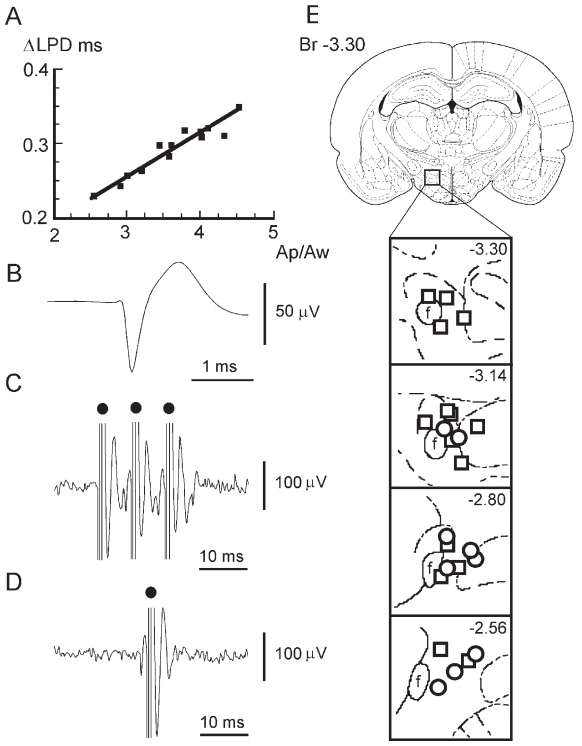

Figure 3. Comparison of LPD Recorded with Micropipettes and Microwires in Antidromically Identified Hcrt Cells and Their Spike Characteristics

(A) Correlation between the difference of LPD (ΔLPD) and amplitude ratio (Ap/Aw) of spikes recorded with micropipette and microwire in anesthetized rats is expressed by linear regression: ΔLPD (ms) = 0.0892 + 0.0558 Ap/Aw; correlation coefficient r = 0.94 (F = 78.2; p < 0.0001; df = 1, 11).

(B) An averaged spike waveform of an Hcrt neuron recorded with microwires in the freely moving rat.

(C) Antidromic spikes of Hcrt neuron to VTA train electrical stimulation in freely moving rat.

(D) Collision of orthodromic and antidromic spikes in axon of Hcrt neuron.

(E) The location of Hcrt (circles) and probable Hcrt (squares) neurons in the PFH and medial LH. Dots, stimulating pulses.

amplitudes of spikes (Figure 3A) recorded with micropipette (Ap) and microwire (Aw). This correlation is linear: ΔLPD = 0.0892 + 0.0558 Ap/Aw (r = 0.94; F = 78.2; p < 0.0001; df = 1, 11). Therefore, an average ΔLPD = 0.29 ms may be determined based on an average amplitude ratio Ap/Aw = 3.6. Thus, using data obtained in the previous experiment with juxtacellular labeling, we can calculate the approximate expected spike LPDs for antidromically and orthodromically excited Hcrt cells as ranging from 0.53 ms to 0.74 ms and from 0.61 ms to 0.88 ms, respectively, during microwire recording.

In our study in urethane-anesthetized animals, the majority of identified Hcrt neurons had spontaneous firing rates comparable to those seen in rodent brain slices (Eggermann et al., 2003; Li et al., 2002). This suggests that urethane anesthesia does not strongly influence the state of the membrane potential relative to that seen in vitro. Our comparison of LPDs of antidromically identified Hcrt neurons confirmed that these spike

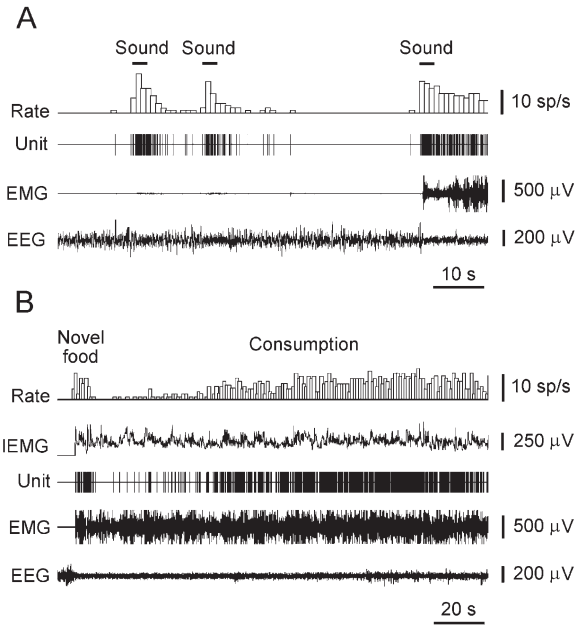

Figure 4. Responses of an Hcrt Neuron to Natural External Stimuli

(A) Sound stimuli induce short-lasting Hcrt cell excitation independently of marked neck muscle activation.

(B) Transient decrease of Hcrt cell activity in response to presentation of novel food (chicken). During decrease of firing rate, rat sniffed, tasted, and backed away from food. Hcrt cell firing accelerated in conjunction with onset of consumption. EMG, neck muscle electromyogram. EEG, electroencephalogram.

parameters did not significantly differ (t = 0.5; p = 0.61) between urethane anesthetized (current experiment) and freely moving rats (see below). Thus, based on the results of this experiment we conclude that the LPD for Hcrt cell spikes exceeds 0.53 ms during recordings with 12.5 μm microwires in freely moving rats.

Unit Recording in Freely Moving Rats

During 308 microwire insertions into the PFH and LH, we found nine neurons that met our criteria for Hcrt cells. They (1) had spike LPD ranging from 0.56 ms to 0.77 ms with a mean of 0.64 ± 0.02 ms (Figure 3B), (2) responded antidromically with an average latency of 4.31 ± 0.18 ms (n = 9; min = 3.5 ms; max = 6.1 ms) during VTA stimulation (Figures 3C and 3D), and (3) were located in the PFH and the medial part of the LH (Figure 3E).

The firing rate of neurons that met the above criteria significantly increased during EEG desynchronization (Figures 4A and 5A) and negatively correlated with EEG spectral powers in delta, theta, alpha, and beta frequency bands (Figures 6A–6D). In the beta frequency band, this correlation was substantially weaker. In contrast, increased Hcrt cell discharge was accompanied by an elevation of EEG spectral power in the gamma frequency band (Figure 6E). During intensive motor activity, the discharge rate of Hcrt neurons further increased and significantly correlated with the amplitude of the neck EMG (Figures 5 and 7A). An average correlation coefficient that reflected the link between the fir-

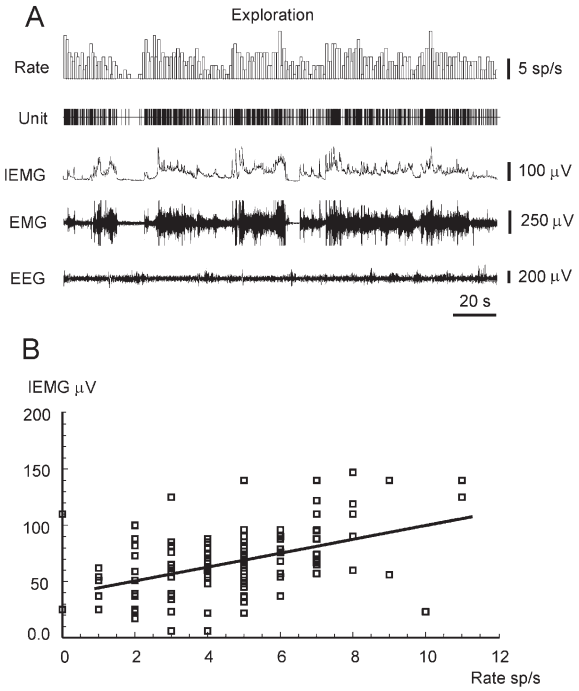

Figure 5. Example of the Correlation between the Firing Rate of an Hcrt Neuron and the Amplitude of the Neck EMG during Exploratory Behavior

(A) The alteration of Hcrt cell firing rate, neck EMG, integrated neck EMG (IEMG), and EEG during exploratory behavior of freely moving rat.

(B) Correlation between Hcrt cell firing rate and the amplitude of the neck IEMG during exploratory behavior is expressed by a linear regression: IEMG (μV) = 39.31 + 6.15 rate (spikes/s); correlation coefficient r = 0.48 (F = 39.8; p < 0.0001; df = 1, 133). See abbreviations in Figure 4.

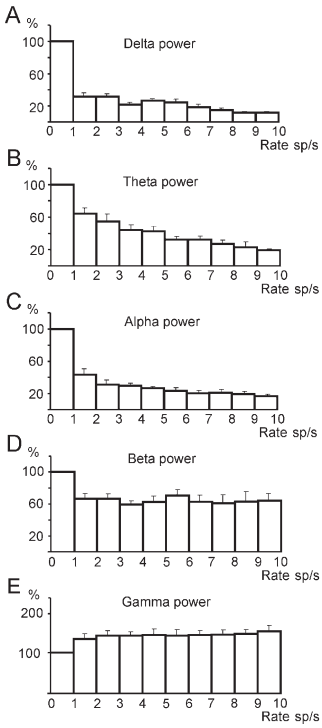

Figure 6. The Alteration of EEG Spectral Power in the Delta, Theta, Alpha, Beta, and Gamma Frequency Bands during Periods of Increased Firing of Hcrt Neurons

(A–C) The decrease of EEG powers in the delta, theta, and alpha frequency bands. Correlation coefficients for exponential regression models: r = –0.69, F = 23.1; r = –0.7, F = 43.7; r = –0.65, F = 19.6; p < 0.0001; df = 1, 65, respectively. (D) Weak correlation between discharge rate of Hcrt neurons and EEG power in beta frequency band (r = –0.29; F = 5.92; p < 0.05; df = 1, 65). (E) The increase of EEG power in gamma frequency band (r = 0.65; F = 53.8; p < 0.0001; df = 1, 65). Figure is based on the analysis of data from nine Hcrt cells. Error bars indicate SEM.

ing rate of identified Hcrt neurons and the amplitude of the neck EMG was 0.42 ± 0.03 (min = 0.26; max = 0.59; n = 9). Although the activity of Hcrt cells was correlated with the presence of motor activity, it was not related to the direction of specific movements and was not modulated by rhythmic movements such as those occurring during grooming or locomotion. Moreover, in some cases, an increased firing rate was observed without substantial motor output. In particular, the lack of correlation between Hcrt cell discharges and EMG amplitude was revealed with sound stimuli that produced EEG desynchronization without substantial neck muscle activation (Figure 4A). Conversely, behaviors that were accompanied by equal levels of motor activity could have very different rates of Hcrt cell discharge. For example, presentation and tasting of a novel food that induced initial food aversion, manifested as repeated approaches and withdrawals, were accompanied by reduced Hcrt cell discharges for an average of 29 ± 4 s (min = 17 s; max = 45 s; n = 7) despite strong EEG desynchronization and the presence of motor activity. During subsequent consumption, Hcrt cell firing rate gradually increased without substantial alteration in EEG or intensity of movements (Figure 4B). In contrast, consumption of a familiar food was accompanied by moderate discharge rates throughout the consumption period. Motor activity appeared similar in these two situations.

Hcrt neurons strongly decreased their firing rates or ceased discharge during quiet wakefulness (QW), and virtually ceased activity in SW sleep as well as in the tonic phase of REM sleep (Figures 7B–7D; Figure 8A). During the phasic periods of REM sleep, the average firing rate of these cells increased and sometimes correlated with spontaneous twitches (Figure 7D).

We also found 15 PFH and LH neurons that were excited orthodromically by VTA stimulation with a latency that ranged from 3 ms to 11 ms. These neurons had LPDs ranging from 0.58 ms to 0.86 ms with a mean of 0.73 ± 0.02 ms (n = 15) in our microwire recordings. As in anesthetized rats, the LPD for the spontaneous spikes of these cells was significantly broader than spike LPDs of identified Hcrt neurons recorded with microwires (t = 3.15; p < 0.005). These probable Hcrt neurons also were located in the PFH and the medial part of the LH (Figure 3E) and showed similar discharge patterns during the S-W cycle. In particular, both identified Hcrt neurons and the probable Hcrt cells that re-

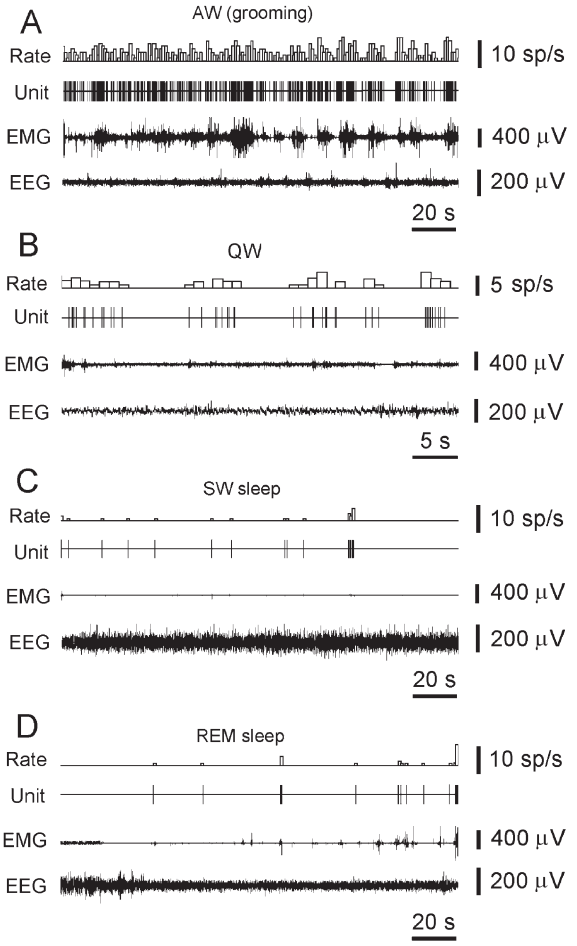

Figure 7. The Discharge Pattern of a Representative Hcrt Neuron across the S-W Cycle in the Freely Moving Rat

(A) High firing rates are seen during AW (grooming).

(B) Reduced firing rate or cessation of activity is seen in QW and drowsiness.

(C) A further decrease or cessation of firing is seen during SW sleep.

(D) Minimal firing rate is seen during the tonic phase of REM sleep. Brief Hcrt cell discharge bursts are correlated with muscle twitches during the phasic events of REM sleep.

sponded orthodromically to VTA stimulation exhibited maximal activity during exploratory behavior and significantly lower firing rates during grooming and eating. Similarly, both cell groups greatly reduced their activity in QW and sleep (Figure 8).

Discussion

Our data show that Hcrt neurons in the rat are maximally active in relation to exploration, with lower levels of discharge during grooming and eating, behaviors that can have more intense electromyographic activity. Hcrt firing rate is minimal in quiet waking and during sleep. Although, in general, Hcrt unit activity is linked to movement and EEG arousal, it can be more or less intense than would be expected from the equivalent movement or EEG changes, during states that appear

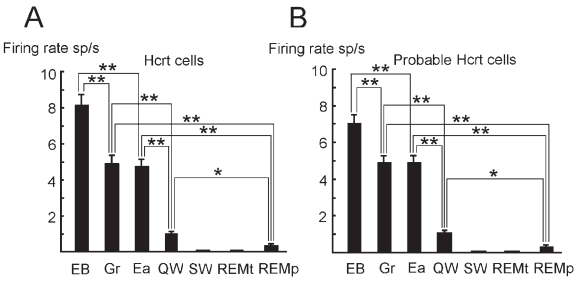

Figure 8. Firing Rate of Hcrt and Probable Hcrt Cells in Waking and Sleep Behaviors in Freely Moving Rats

Exploratory behavior (EB), grooming (Gr), eating (Ea), QW, SW sleep (SW), and tonic (REMt) and phasic (REMp) sleep. Maximal discharge is seen during exploration-approach behavior. (A) Discharge pattern of Hcrt neurons (n = 9). (B) Discharge pattern of probable Hcrt neurons (n = 15) orthodromically excited by VTA stimulation. Bonferroni t test, *$p < 0.05$, **$p < 0.01$. Error bars indicate SEM.

to have strong emotional components. The methodological approach that we have developed for identification of these cells in behaving animals should have broad applicability to further studies of the behavioral and emotional determinants of Hcrt discharge with high temporal resolution.

Methodological Considerations

We found that Hcrt neurons located in the PFH and the medial part of the LH have projections to the VTA and in turn receive excitatory inputs from this area. Hcrt neurons excited antidromically and orthodromically during VTA stimulation had spikes with longer-duration LPDs than adjacent hypothalamic cells. Our results show that using the LPD as criterion for antidromic spikes provides practically unerring identification of Hcrt neurons that send axons to the VTA. We also found that Hcrt neurons innervating the LC have a similar LPD duration and are located in the PFH and dorsal part of the LH.

How representative are the identified Hcrt cells in the present study of the entire Hcrt population? All of the cells that we identify on the basis of waveform and projection had the same profile of sleep-waking discharge, with maximum discharge in AW and minimal activity in SW and REM sleep, a pattern not seen in hypothalamic cells with shorter spike durations. They also showed the same pattern of activity change with feeding, grooming, and exploratory behavior. The Hcrt cells that we have described are located in the PFH and medial portion of the LH. More than 50% of the Hcrt cell population is in this region (Espana et al., 2005; Peyron et al., 1998; Thannickal et al., 2000). In vitro work has not identified any physiological difference between subgroups of Hcrt cells within the Hcrt field.

Most Hcrt cells have multiple axonal projections to widespread regions of the brain. For example, individual cells project to both LC and forebrain structures (Espana et al., 2005). Thus, it is likely that cells identified by VTA or LC stimulation would overlap with those that might be activated with stimulation elsewhere in

the Hcrt axonal projection fields. Such overlapping and widespread projection patterns are most compatible with a uniform activity pattern of Hcrt cells. The other diffusely projecting cell groups to which Hcrt cells most strongly and reciprocally interconnect (e.g., the serotonin, norepinephrine, and histamine cells) have each been shown to have relatively homogeneous sleep cycle and behavioral correlates of discharge, with cessation of activity in REM sleep and increased activity during waking motor activity. The finding that cells with long-duration action potentials throughout the Hcrt cell region are off in REM sleep and active in waking (Alam et al., 2002; Koyama et al., 2003) also supports the hypothesis that the medial, central, and lateral Hcrt populations have similar behavioral roles.

Thus, the anatomical and physiological evidence suggests that the Hcrt cell population identified in the present study may be representative of the entire Hcrt cell population. Nevertheless, it remains possible that some minority of cells within the Hcrt field have differing patterns of discharge from that which we observed in all the identified Hcrt cells.

Behavioral Correlates of Hcrt Cell Activity during Wakefulness

In our experiments, unit recording in freely moving rats revealed that the firing rate of antidromically identified Hcrt neurons is negatively correlated with EEG spectral power in the delta, theta, alpha, and beta frequency bands in the prefrontal cortex. On the other hand, Hcrt cell firing rate was positively correlated with EEG power in the gamma band. It has been shown that similar EEG alterations are correlated with an increase of norepinephrine and dopamine release in this cortical region (Chang et al., 1995; Luoh et al., 1994). Hcrt-induced cortical arousal may be mediated through ascending monoaminergic (Brown et al., 2001; Brown et al., 2002; Horvath et al., 1999; Huang et al., 2001; Liu et al., 2002; Wisor et al., 2001) and cholinergic systems (Burlet et al., 2002; Eggermann et al., 2001; Espana et al., 2001) as well as through reticular and thalamocortical systems (Lambe and Aghajanian, 2003) and direct cortical projections (Fadel et al., 2002; Nambu et al., 1999; Peyron et al., 1998).

Our experiments also demonstrated that motor activity in freely moving animals is generally accompanied by activation of Hcrt neurons. However, no obvious difference in discharge rate was seen in movements to the ipsilateral versus contralateral side or in the dorsal versus ventral directions, in contrast to the behavioral correlates of midbrain, pontine, and medullary reticular neurons (Siegel, 1979; Siegel and McGinty, 1978; Siegel and Tomaszewski, 1983). It has been shown that stimulation of the PFH and LH induces motor activation and exploration (Valenstein, 1971; Valenstein et al., 1970). Such stimulation also elicits coordinated extension of hindlimb and neck muscles along the sagittal plane when a rat prepares to step (Sinnamon and Polania, 1997). Lesions of this region lead to a profound akinesia (Levitt and Teitelbaum, 1975). These results together suggest that Hcrt cells link arousal and motor activity.

However, our data show that Hcrt neurons may respond with burst discharge to sensory stimuli without concomitant motor activation. It remains to be determined if sensory stimulation by itself will elicit unit discharge or if only sensory stimulation that attracts the interest of the animal will be linked to elevated discharge rates. It also remains to be determined if stimuli heralding an aversive situation will produce the same response as stimuli heralding a positively reinforcing situation.

The elevated activity of Hcrt cells during exploration might be explained by increased vigilance to the environment during this behavior, as appears to be the case with LC cells (Aston-Jones et al., 1991) that receive strong Hcrt innervations (Peyron et al., 1998). However, we found that Hcrt cell firing decreases during food aversion, a state characterized by high levels of attention to threatening stimuli, strong EEG desynchronization, and the presence of high levels of motor activity. Thus, these data suggest that emotional states modulate the activity of Hcrt neurons.

In this respect, Hcrt cell activation appears to be correlated with the sorts of behavior that trigger cataplexy in narcoleptics. Human cataplexy is most frequently elicited by laughter, which produces a slight weakness in normal individuals (Guilleminault, 1976). Sadness and pain do not usually trigger cataplexy even when they are accompanied by increased motor activity and cortical arousal. In narcoleptic dogs, cataplexy is triggered by the consumption of highly palatable food and excited play, but not by moderately palatable food, not by noxious stimuli, and not in unfamiliar environments even if the dogs are highly aroused and active (Baker and Dement, 1985; John et al., 2004; Mitler et al., 1976; Siegel, 2000; Siegel et al., 1991). In rodents, cataplexy is most frequently linked to exploration, burrowing, and investigation of the environment (Chemelli et al., 1999; Hara et al., 2001). Thus, the behavioral situations most frequently occurring prior to rodent cataplexy are those that we found to be associated with the highest levels of Hcrt unit discharge. We hypothesize that Hcrt neurons are important part of an "approach-exploratory" system that is involved in maintaining muscle tone and regulating motor activity (Siegel, 2004). In the absence of normal numbers of Hcrt cells, Hcrt receptor-2, or Hcrt synthesis, muscle tone cannot be sustained during the strong activation of this system, and waking cannot be maintained for long periods in the absence of sensory stimulation. It is also likely that long-term responses to the loss of hypocretin cells such as up- and downregulation of receptors and related physiological responses may contribute to the symptoms of narcolepsy.

Spontaneous Hcrt Cell Activity in QW and Sleep

We could find Hcrt and putative Hcrt neurons in the PFH and LH of freely moving animals only in the presence of arousing stimuli. In contrast, some data obtained during intracellular recording of identified Hcrt neurons in brain slices demonstrate that Hcrt cells are in a depolarized state that promotes their spontaneous activity (Eggermann et al., 2003; Li et al., 2002). On the other hand, it has been shown that the $GABA_A$ agonist muscimol, serotonin, and norepinephrine application hyperpolarize the membrane of Hcrt neurons and block

their spontaneous discharge (Li et al., 2002; Li and van den Pol, 2005). Although glutamate and Hcrt evoke depolarization and increase the firing rate of Hcrt neurons (Eggermann et al., 2003; Li et al., 2002; Yamanaka et al., 2003), their excitatory action is substantially attenuated by group III metabotropic glutamate receptors that maintain a tonic inhibition of excitatory synaptic input to Hcrt neurons (Acuna-Goycolea et al., 2004). Neuropeptide Y strongly inhibits the activity of Hcrt cells via multiple presynaptic and postsynaptic mechanisms (Fu et al., 2004). Thus, these data suggest that the inhibitory influence on Hcrt neurons may be predominant in intact, quiescent, unanesthetized animals.

Our studies of Hcrt cell activity across the S-W cycle showed that these cells have maximal firing rates during AW and reduce activity during QW, SW, and REM sleep. A similar discharge pattern was observed across the S-W cycle during the recording of Hcrt neurons that were juxtacellularly labeled in a head-restrained rat (Lee and Jones, 2004). c-Fos studies also demonstrated that the number of Hcrt+/c-Fos+ neurons was maximal during AW and decreased during QW and sleep (Estabrooke et al., 2001; Torterolo et al., 2003; Torterolo et al., 2004). Thus, the behavioral correlates of Hcrt neuron discharges have some similarities to those of the norepinephrine (Aston-Jones et al., 1994; Aston-Jones et al., 2001), serotonin (Fornal et al., 1996; Jacobs, 1991; Veasey et al., 1997), and histamine (Chu et al., 2004; John et al., 2004; Vanni-Mercier et al., 2003) cells to which Hcrt cells are reciprocally connected. However, unlike these monoaminergic cells that show tonic activity in QW, Hcrt cells are often completely silent during behavioral quiescence in waking. During AW, the discharge of Hcrt cells is irregular and related to behavior, whereas most monoaminergic cells show a regular discharge pattern. Finally, monoaminergic cells show significantly higher discharge rates in SW sleep than in REM sleep, but Hcrt cells are essentially inactive in both states.

Our previous microdialysis studies demonstrated that the level of Hcrt release is significantly higher in AW relative to QW and SW sleep in freely moving cats. However, REM sleep was accompanied by elevated Hcrt levels in the hypothalamus and basal forebrain relative to SW sleep levels (Kiyashchenko et al., 2002). It is well known that neurotransmitter release does not necessarily correlate with cellular activity across the S-W cycle. In particular, Cespuglio (Cespuglio et al., 1990; Cespuglio et al., 1992) has shown that serotonin release is maximal within the dorsal raphe during REM sleep, even though serotonergic cells have their lowest levels of discharge and terminal release of serotonin outside the nucleus in REM sleep (Houdouin et al., 1991; Portas and McCarley, 1994; Trulson and Jacobs, 1979). Similarly, dopaminergic release in some brain regions is modulated independently from the discharge of dopaminergic cells (Borland and Michael, 2004; Mathe et al., 1999). We hypothesize that Hcrt cells, like monoaminergic neurons, have both spike-dependent and spike-independent neurotransmitter release.

Conclusion

We hypothesize that identified Hcrt neurons are involved in the regulation of motivational and/or emotional aspects of behavior-modulating motor activity and cortical arousal. The malfunction of such modulation would be consistent with the symptoms resulting from the loss of Hcrt cells in human and animal narcoleptics, particularly the inability to maintain waking arousal and the losses of muscle tone during cataplectic attacks induced by emotional stimuli. The anatomical links between Hcrt neurons and monoaminergic and cholinergic nuclei as well as limbic structures can mediate this proposed modulatory function.

Experimental Procedures

Animals

Experiments were done in 62 male Wistar rats weighing 250–300 g. Forty-four rats were anesthetized and used for juxtacellular labeling PFH and LH neurons with subsequent immunostaining. Four anesthetized animals were used for simultaneous recording with micropipettes and microwires. Fourteen rats were operated on for polygraphic determination of S-W states and unit recording in chronic experiments in unrestrained, unanesthetized rats. All procedures were performed in accordance with the National Research Council Guide for the Care and Use of Laboratory Animals and were approved by the Animal Research Committees of the University of California at Los Angeles and of the Veterans Administration Greater Los Angeles Healthcare system.

Surgery

For acute experiments, rats were anesthetized with urethane (1.8–2.5 g/kg, i.p.), and a rectangular hole was cut through the skull bone. The transverse anterior and posterior borders of this opening were located 2 and 7 mm posterior to bregma (Br) with symmetrical lateral borders 3 mm from the midline. One hole with diameter 0.5 mm was drilled into the rostral frontal bone for a reference electrode.

For chronic experiments, anesthesia was induced with ketamine/xylazine injection (75 mg/kg and 5 mg/kg, i.p.) followed by maintenance on gas (isoflurane 0.5%–1.0%) anesthesia. Prefrontal cortical electroencephalographic and dorsal neck EMG electrodes were implanted aseptically for polygraphic determination of the S-W states. The Teflon base with guide cannula was fixed on the skull such that the cannula tip was positioned 3 mm above the dorsal aspect of the PFH (Br = –3.14 mm, L = 1.3 mm, H = 8.3 mm). Bipolar stimulating electrodes were implanted in the ipsilateral VTA (Br = –5.6, L = 0.5, H = 8.5) or LC (Br = –9.80, L = 1.3, H = 7.4). Coordinates were determined with the rat brain atlas of Paxinos and Watson (1997). Experiments were carried out after allowing a minimum of 7 days for recovery from surgery.

Recording and Electrical Stimulation

In acute experiments, extracellular unit recording, and juxtacellular labeling were performed with glass micropipettes with a tip diameter of 1.0–1.5 μm (Pinault, 1996). Monitoring of extracellular unit activity and juxtacellular iontophoresis was performed through the bridge input circuit of an Axoclamp-2A connected to an A-M systems amplifier (model 1700), both during the injection period and 5 min after injection, to ensure that the neuron remained alive.

Sixteen micropipette insertions were performed on each brain side from Br = –2.20 mm to Br = –3.4 mm and from L = 0.6 mm to L = 1.8 mm. The distance between the micropipette insertions was about 300 μm. Unit recording and juxtacellular labeling were performed only for well-isolated single PFH and LH neurons that had signal/noise ratio greater than 7:1. This signal/noise ratio provided successful juxtacellular labeling of only single neurons. In anesthetized rats, spontaneous and evoked firing rates were calculated for 10 s intervals. Ten intervals were used for statistical analysis.

To estimate the alteration of spike LPD during transition from micropipette to microwire recording of Hcrt cells, simultaneous registration of antidromic spikes was carried out with composite electrodes in anesthetized rats. For this purpose, microwires (diameter 12.5 μm) were glued to glass micropipettes (tip 1.0–1.5 μm) with a distance between the tips of 20–30 μm to allow simulta-

neous recordings from antidromically identified Hcrt cells. Glass micropipettes were stretched asymmetrically to glue the microwire to the pipette (see Figure S1 in the Supplemental Data available with this article online).

In chronic experiments, unit recording was carried out with a microdrive, equipped with seven microwires (diameter 12.5 μm). The design of the microdrive allowed multiple microwire insertions in the brain. The distance between microwire tips was about 300 μm. The microdrive was fixed on a Teflon base before unit recording. Only units with signal/noise ratio more than 3:1 were used. Analog signals from microwires and EEG and EMG electrodes were amplified with an A-M system amplifier (model 1700) and Grass polygraph (model 78 D), digitized, and displayed on a computer monitor with an integrated computer interface device and software (CED1401 Plus; Spike2 software; Cambridge Electronic Design).

Rats were maintained on 12 hr:12 hr light-dark cycle (lights on 08.00 hr) with food and water freely available. During the recovery period, animals were placed for 3–4 hr per day in an electrically shielded, sound-attenuated recording chamber (temperature, 25°C ± 2°C) for adaptation to the recording conditions. Assessment of S-W states was based on EEG and neck EMG patterns. During AW and QW, a desynchronized EEG was accompanied by variable high-amplitude or stable low-amplitude EMG. SW sleep was identified by the presence of high-voltage slow waves and spindles. The tonic phase of REM sleep was distinguished by EEG desynchronization and the disappearance of EMG signals. Phasic REM stage was accompanied by EMG bursts that corresponded to muscle twitches.

Constant-current square-wave pulses were delivered through bipolar stimulating electrodes (stainless steel, 100 μm) by the use of an S88 stimulator (Grass Instruments) coupled with a stimulus isolation unit (TF5S21ZZ). Bipolar electrode tips were separated by 0.8–1.0 mm. PFH cell spikes were determined to be antidromic if they met the following criteria during VTA stimulation: (1) stimulation of ipsilateral VTA (0.2 ms, 300–800 μA, trains of three pulses at frequency of >100 Hz) produced antidromic spikes at an invariant latency of <±0.2 ms, and (2) collision of antidromic spikes with spontaneous spikes could be demonstrated.

Juxtacellular Labeling and Immunostaining

Nb (Vector Laboratories Inc., Burlingame, CA) dissolved at 4% in 0.5 M CH_3COOK was delivered through glass micropipettes. The micropipette was advanced slowly toward the neuron, with a hydraulic microdrive (Trent Wells Inc., South Gate, CA) until it was possible to modulate its firing by current pulses with an amplitude of 0.5–4.0 nA and duration 200 ms (Pinault, 1996). Only cells with similar electrophysiological characteristics were labeled on each side of the brain.

Two to five hours after the end of the labeling, the rat received a lethal dose of pentobarbital and was perfused transcardially with heparinized 0.1 M phosphate buffer (PB) (pH 7.4), followed by 4% paraformaldehyde in 0.1 M PB. The brain was removed, post-fixed ice-cold in the same fixative for 12 hr and immersed in 30% sucrose for 48 hr. Brain pieces that contained PFH were dissected and stored at –80°C. Forty micrometer thick sections were sliced with a cryostat. After a rinse with Tris-NaCl (pH 7.4), sections were incubated for 24 hr at room temperature in a primary antibody mixture of goat polyclonal IgG against Hcrt-1, and a rabbit polyclonal IgG against MCH (dilution at 1:200; Santa Cruz Biotechnology, Santa Cruz, CA). After a second rinse, sections were incubated for 3 hr in a secondary antibody mixture of an anti-goat IgG-Cy3, anti-rabbit IgG-7-amino-4-methylcoumarin-3-acetic acid, and Cy2-conjugated streptavidin (dilutions at 1:200 for all antibodies; Jackson ImmunoResearch, West Grove, PA). Mounted sections were investigated under a fluorescent microscope (Eclipse E600, Nikon, Japan). Nb-filled neurons were seen in green, Hcrt-1-positive cells were seen in red, and MCH-positive cells were seen in blue. Specificity for Hcrt or MCH staining was demonstrated by preabsorption of the antiserum with the appropriate peptide.

Search for Hcrt Neurons in Freely Moving Animals

High-frequency electrical train stimulation of the VTA evoked strong exploratory behavior followed by grooming in freely moving rats. Intensive motor activity frequently resulted in a reduction of signal/noise ratio, presumably due to microelectrode displacement. Therefore, antidromic identification of presumed Hcrt cells (spike LPD > 0.53 ms) was performed after the study of their discharge patterns across the S-W cycle. Because QW is characterized by few Hcrt+/c-Fos+ neurons (Espana et al., 2003; Torterolo et al., 2004), we used white noise (90–110 dB, 5–10 s), food smells, and an air stream with mice bedding smell as arousing stimuli to find Hcrt cells during unit recording.

Data Analysis

Test for homogeneity of variances showed that LPD variances for Hcrt ($V = 0.013$; $n = 26$) and non-Hcrt ($V = 0.005$; $n = 34$) cells were significantly less than variances for spike durations for Hcrt ($V = 0.04$; $n = 26$) and non-Hcrt neurons ($V = 0.05$; $n = 34$) during recording with micropipettes in urethane anesthetized rats (Bartlett's chi-square = 49.5; $p < 0.0001$). Decreased signal to noise ratios during recording with microwires in freely moving animals makes the exact determination of spike duration between initial and final points difficult. Therefore, we used the LPD as a more stable parameter that reflects the duration of the intracellular afterhyperpolarization phase (Henze et al., 2000), which is important for identification of Hcrt cells, and the total width of hypothalamic cell spikes. Ten spikes were measured for Ap, Aw, and LPD for each antidromically identified cell recorded with micropipette and microwire. The means of parameters for each neuron were used for regression analysis.

The Neurolucida computer-aided plotting system (MicroBrightField) was utilized for marking the location of Nb-filled neurons alone, and also the cells exhibiting combined staining for Nb + Hcrt. Individual section outlines were drawn at 2–10× magnifications, and the classification and mapping of double-stained neurons were performed under 100× magnification.

In anesthetized rats, spontaneous and evoked firing rates were calculated for 10 s intervals. Ten intervals were used for statistical analysis. In freely moving animals, electrophysiologically identified Hcrt cells were recorded across at least two S-W cycles (AW, QW, SW sleep, and REM sleep). EEG spectral analysis was performed on 5 s episodes with Spike2 software in delta (0.1–3 Hz), theta (4–8 Hz), alpha (8–12 Hz), beta (13–30 Hz), and gamma (30–75 Hz) frequency bands. Integration of the EMG signal was carried out with Spike2 software using a low-frequency roll off of 10 Hz.

To determine the location of recorded cells, cathodal currents (25–40 μA, 20–30 s) were passed through the microwires at the end of the tracks. After the final experiment, the marking lesion was placed at the point of the last unit recording. The brain sections were subjected to immunostaining, and the location of recorded neurons was determined by using the track made by microwires, depth of the marking lesions, and depth measurements on the microdrive. The electrode lesions were identified on a Nikon microscope and plotted with a Neurolucida interface according to the atlas of Paxinos and Watson (1997). ANOVA, Bonferroni t test, regression analysis, paired Student's t test, and test for homogeneity of variances were used for statistical analysis. All values are given as the mean ± SEM.

Supplemental Data

The Supplemental Data include one supplemental figure and can be found with this article online at http://www.neuron.org/cgi/content/full/46/5/787/DC1/.

Acknowledgments

Grant support provided by US National Institutes of Health (NS14610, MH071350, and MH064109) and the Medical Research Service of the Department of Veterans Affairs. Related work is available at http://www.npi.ucla.edu/sleepresearch.

Received: December 28, 2004
Revised: March 22, 2005
Accepted: April 28, 2005
Published: June 1, 2005

References

Acuna-Goycolea, C., Li, Y., and van den Pol, A.N. (2004). Group III metabotropic glutamate receptors maintain tonic inhibition of excitatory synaptic input to hypocretin/orexin neurons. J. Neurosci. *24*, 3013–3022.

Alam, M.N., Gong, H., Alam, T., Jaganath, R., McGinty, D., and Szymusiak, R. (2002). Sleep-waking discharge patterns of neurons recorded in the rat perifornical lateral hypothalamic area. J. Physiol. *538*, 619–631.

Aston-Jones, G., Chiang, C., and Alexinsky, T. (1991). Discharge of noradrenergic locus coeruleus neurons in behaving rats and monkeys suggests a role in vigilance. Prog. Brain Res. *88*, 501–520.

Aston-Jones, G., Rajkowski, J., Kubiak, P., and Alexinsky, T. (1994). Locus coeruleus neurons in monkey are selectively activated by attended cues in a vigilance task. J. Neurosci. *14*, 4467–4480.

Aston-Jones, G., Chen, S., Zhu, Y., and Oshinsky, M.L. (2001). A neural circuit for circadian regulation of arousal. Nat. Neurosci. *4*, 732–738.

Baker, T.L., and Dement, W.C. (1985). Canine narcolepsy-cataplexy syndrome: Evidence for an inherited monoaminergic-cholinergic imbalance. In Brain Mechanisms of Sleep, D.J. McGinty, R. Drucker-Colin, A. Morrison, and P.L. Parmeggiani, eds. (New York: Raven Press), pp. 199–234.

Bayer, L., Eggermann, E., Serafin, M., Saint-Mleux, B., Machard, D., Jones, B., and Muhlethaler, M. (2001). Orexin (hypocretin) directly excite tuberomammillary neurons. Eur. J. Neurosci. *14*, 1571–1575.

Beyer, C., Alamanza, J., DelaTorre, L., and Guzmanflores, C. (1971). Brain stem multi-unit activity during 'relaxation' behavior in the female cat. Brain Res. *29*, 213–222.

Borland, L.M., and Michael, A.C. (2004). Voltammetric study of the control of striatal dopamine release by glutamate. J. Neurochem. *91*, 220–229.

Brown, R.E., Sergeeva, O., Eriksson, K.S., and Haas, H.L. (2001). Orexin A excites serotonergic neurons in the dorsal raphe nucleus of the rat. Neuropharmacology *40*, 457–459.

Brown, R.E., Sergeeva, O.A., Eriksson, K.S., and Haas, H.L. (2002). Convergent excitation of dorsal raphe serotonin neurons by multiple arousal systems (orexin/hypocretin, histamine and noradrenaline). J. Neurosci. *22*, 8850–8859.

Burlet, S., Tyler, C.J., and Leonard, C.S. (2002). Direct and indirect excitation of laterodorsal tegmental neurons by Hypocretin/Orexin peptides: implications for wakefulness and narcolepsy. J. Neurosci. *22*, 2862–2872.

Cespuglio, R., Sarda, N., Gharib, A., Chastrette, N., Houdouin, F., Rampin, C., and Jouvet, M. (1990). Voltammetric detection of the release of 5-hydroyindole compounds throughout the sleep-waking cycle of the rat. Exp. Brain Res. *80*, 121–128.

Cespuglio, R., Houdouin, F., Oulerich, M., El Mansari, M., and Jouvet, M. (1992). Axonal and somato-dendritic modalities of serotonin release: their involvement in sleep preparation, triggering and maintenance. J. Sleep Res. *1*, 150–156.

Chang, A.Y., Kuo, T.B., Tsai, T.H., Chen, C.F., and Chan, S.H. (1995). Power spectral analysis of electroencephalographic desynchronization induced by cocaine in rats: correlation with evaluation of noradrenergic neurotransmission at the medial prefrontal cortex. Synapse *21*, 149–157.

Chemelli, R.M., Willie, J.T., Sinton, C., Elmquist, J., Scammell, T., Lee, C., Richardson, J., Williams, S., Xiong, Y., Kisanuki, Y., et al. (1999). Narcolepsy in *orexin* knockout mice: Molecular genetics of sleep regulation. Cell *98*, 437–451.

Chu, M., Huang, Z.L., Qu, W.M., Eguchi, N., Yao, M.H., and Urade, Y. (2004). Extracellular histamine level in the frontal cortex is positively correlated with the amount of wakefulness in rats. Neurosci. Res. *49*, 417–420.

de Lecea, L., Kilduff, T.S., Peyron, C., Gao, X., Foye, P.E., Danielson, P.E., Fukuhara, C., Battenberg, E.L., Gautvik, V.T., Bartlett, F.S., II, et al. (1998). The hypocretins: hypothalamus-specific peptides with neuroexcitatory activity. Proc. Natl. Acad. Sci. USA *95*, 322–327.

Eggermann, E., Serafin, M., Bayer, L., Machard, D., Saint-Mleux, B., Jones, B.E., and Muhlethaler, M. (2001). Orexins/hypocretins excite basal forebrain cholinergic neurones. Neuroscience *108*, 177–181.

Eggermann, E., Bayer, L., Serafin, M., Saint-Mleux, B., Bernheim, L., Machard, D., Jones, B.E., and Muhlethaler, M. (2003). The wake-promoting hypocretin-orexin neurons are in intrinsic state of membrane depolarization. J. Neurosci. *23*, 1557–1562.

Espana, R.A., Baldo, B.A., Kelley, A.E., and Berridge, C.W. (2001). Wake-promoting and sleep-suppressing actions of hypocretin (orexin): basal forebrain sites of action. Neuroscience *106*, 699–715.

Espana, R.A., Valentino, R.J., and Berridge, C.W. (2003). Fos immunoreactivity in hypocretin-synthesizing and hypocretin-1 receptor-expressing neurons: effects of diurnal and nocturnal spontaneous waking, stress and hypocretin-1 administration. Neuroscience *121*, 201–217.

Espana, R.A., Reis, K.M., Valentino, R.J., and Berridge, C.W. (2005). Organization of hypocretin/orexin efferents to locus coeruleus and basal forebrain arousal-related structures. J. Comp. Neurol. *481*, 160–178.

Estabrooke, I.V., McCarthy, M.T., Ko, E., Chou, T.C., Chemelli, R.M., Yanagisawa, M., Saper, C.B., and Scammell, T.E. (2001). Fos expression in orexin neurons varies with behavioral state. J. Neurosci. *21*, 1656–1662.

Fadel, J., and Deutch, A.Y. (2002). Anatomical substrates of orexin-dopamine interactions: lateral hypothalamic projections to the ventral tegmental area. Neuroscience *111*, 379–387.

Fadel, J., Bubser, M., and Deutch, A.Y. (2002). Differential activation of orexin neurons by antipsychotic drugs associated with weight gain. J. Neurosci. *22*, 6742–6746.

Findlay, A.L.R., and Hayward, J.N. (1969). Spontaneous activity of single neurons in the hypothalamus of rabbits during sleep and waking. J. Physiol. *201*, 237–258.

Fornal, C.A., Metzler, C.W., Marrosu, F., Ribiero-do-Valle, L.E., and Jacobs, B.L. (1996). A subgroup of dorsal serotonergic neurons in the cat is strongly activated during oral-buccal movements. Brain Res. *716*, 123–133.

Fu, L.Y., Acuna-Goycolea, C., and van den Pol, A.N. (2004). Neuropeptide Y inhibits hypocretin/orexin neurons by multiple presynaptic and postsynaptic mechanisms: tonic depression of the hypothalamic arousal system. J. Neurosci. *24*, 8741–8751.

Glotzbach, S.F., Cornett, C.M., and Heller, H.C. (1987). Activity of suprachiasmatic and hypothalamic neurons during sleep and wakefulness in the rat. Brain Res. *419*, 279–286.

Guilleminault, C. (1976). Cataplexy. In Narcolepsy, C. Guilleminault, W.C. Dement, and P. Passouant, eds. (New York: Spectrum), pp. 125–143.

Hara, J., Beuckmann, C.T., Nambu, T., Willie, J.T., Chemelli, R.M., Sinton, C.M., Sugiyama, F., Yagami, K., Goto, K., Yanagisawa, M., and Sakurai, T. (2001). Genetic ablation of orexin neurons in mice results in narcolepsy, hypophagia, and obesity. Neuron *30*, 345–354.

Henze, D.A., Borhegyi, Z., Csicsvari, J., Mamiya, A., Harris, K.D., and Buzsaki, G. (2000). Intracellular features predicted by extracellular recordings in the hippocampus in vivo. J. Neurophysiol. *84*, 390–400.

Horvath, T.L., Peyron, C., Diano, S., Ivanov, A., Aston-Jones, G., Kilduff, T.S., and van den Pol, A.N. (1999). Hypocretin (orexin) activation and synaptic innervation of the locus coeruleus noradrenergic system. J. Comp. Neurol. *415*, 145–159.

Houdouin, F., Cespuglio, R., and Jouvet, M. (1991). Effects induced by the electrical stimulation of the nucleus raphe dorsalis upon hypothalamic release of 5-hydroxyindole compounds and sleep parameters in the rats. Brain Res. *565*, 48–56.

Huang, Z.L., Qu, W.M., Li, W.D., Mochizuki, T., Eguch, N., Watanabe, T., Urade, Y., and Hayaishi, O. (2001). Arousal effect of orexin

A depends on activation of the histaminergic system. Proc. Natl. Acad. Sci. USA *98*, 9965–9970.

Izumi, T. (1968). Single cell activities of the ventromedial nucleus of the hypothalamus in unanesthetized and unrestrained cats. Seishin Shinkeigaku Zasshi *70*, 493–502.

Jacobs, B.L. (1991). Serotonin and behavior: emphasis on motor control. J. Clin. Psychiatry Suppl. *52*, 17–23.

John, J., Wu, M.-F., Boehmer, L.N., and Siegel, J.M. (2004). Cataplexy-active neurons in the posterior hypothalamus: implications for the role of histamine in sleep and waking behavior. Neuron *42*, 619–634.

Kiyashchenko, L.I., Mileykovskiy, B.Y., Maidment, N., Lam, H.A., Wu, M.F., John, J., Peever, J., and Siegel, J.M. (2002). Release of hypocretin (orexin) during waking and sleep states. J. Neurosci. *22*, 5282–5286.

Korotkova, T.M., Sergeeva, O.A., Eriksson, K.S., Haas, H.L., and Brown, R.E. (2003). Excitation of ventral tegmental area dopaminergic and nondopaminergic neurons by orexins/hypocretins. J. Neurosci. *23*, 7–11.

Koyama, Y., Takahashi, K., and Kayama, Y. (2003). State-dependent activity of neurons in the perifornical hypothalamic area during sleep and waking. Neuroscience *119*, 1209–1219.

Lambe, E.K., and Aghajanian, G.K. (2003). Hypocretin (orexin) induces calcium transients in single spines postsynaptic to identified thalamocortical boutons in prefrontal slice. Neuron *40*, 139–150.

Lee, M., and Jones, B.E. (2004). Discharge of identified orexin neurons across the sleep-waking cycle. Program No. 841.1. Abstract Viewer/Itinerary Planner. (Washington, DC: Society for Neuroscience).

Levitt, D.R., and Teitelbaum, P. (1975). Somnolence, akinesia, and sensory activation of motivated behavior in the lateral hypothalamic syndrome. Proc. Natl. Acad. Sci. USA *72*, 2819–2823.

Li, Y., and van den Pol, A.N. (2005). Direct and indirect inhibition by catecholamines of hypocretin/orexin neurons. J. Neurosci. *25*, 173–183.

Li, Y., Gao, X.B., Sakurai, T., and van den Pol, A.N. (2002). Hypocretin/orexin excites hypocretin neurons via a local glutamate neuron—a potential mechanism for orchestrating the hypothalamic arousal system. Neuron *36*, 1169–1181.

Lin, L., Faraco, J., Kadotani, H., Rogers, W., Lin, X., Qui, X., de Jong, P., Nishino, S., and Mignot, E. (1999). The REM sleep disorder canine narcolepsy is caused by a mutation in the hypocretin (orexin) receptor gene. Cell *98*, 365–376.

Liu, R.J., van den Pol, A.N., and Aghajanian, G.K. (2002). Hypocretins (orexins) regulate serotonin neurons in the dorsal raphe nucleus by excitatory direct and inhibitory indirect actions. J. Neurosci. *22*, 9453–9464.

Luoh, H.F., Kuo, T.B., Chan, S.H., and Pan, W.H. (1994). Power spectral analysis of electroencephalographic desynchronization induced by cocaine in rats: correlation with microdialysis evaluation of dopaminergic neurotransmission at the medial prefrontal cortex. Synapse *16*, 29–35.

Mathe, J.M., Nomicos, G.G., Blakeman, K.H., and Svensson, T.H. (1999). Differential actions of dizocilpine (MK-801) on the mesolimbic and mesocortical dopamine systems: role of neuronal activity. Neuropharmacology *38*, 121–128.

Mitler, M.M., Soave, O., and Dement, W.C. (1976). Narcolepsy in seven dogs. J. Am. Vet. Med. Assoc. *168*, 1036–1038.

Nambu, T., Sakurai, T., Mizukami, K., Hosoya, Y., Yanagisawa, M., and Goto, K. (1999). Distribution of orexin neurons in the adult rat brain. Brain Res. *827*, 243–260.

Parmeggiani, P.L., Cevolani, D., Azzaroni, A., and Ferrari, G. (1987). Thermosensitivity of anterior hypothalamic-preoptic neurons during the waking-sleeping cycle: a study in brain functional states. Brain Res. *415*, 79–89.

Paxinos, G., and Watson, C. (1997). The Rat Brain in Stereotaxic Coordinates (New York: Academic Press).

Peyron, C., Tighe, D.K., van den Pol, A.N., de Lecea, L., Heller, H.C., Sutcliffe, J.G., and Kilduff, T.S. (1998). Neurons containing hypocretin (orexin) project to multiple neuronal systems. J. Neurosci. *18*, 9996–10015.

Peyron, C., Faraco, J., Rogers, W., Ripley, B., Overeem, S., Charnay, Y., Nevsimalova, S., Aldrich, M., Reynolds, D., Albin, R., et al. (2000). A mutation in a case of early onset narcolepsy and a generalized absence of hypocretin peptides in human narcoleptic brains. Nat. Med. *6*, 991–997.

Pinault, D. (1996). A novel single-cell staining procedure performed in vivo under electrophysiological control: morpho-functional features of juxtacellular labeled thalamic cells and other central neurons with biotin or Neurobiotin. J. Neurosci. Methods *65*, 113–136.

Portas, C.M., and McCarley, R.M. (1994). Behavioral state-related changes of extracellular serotonin concentration in the dorsal raphe nucleus: a microdialysis study in the freely moving cat. Brain Res. *648*, 306–312.

Ripley, B., Overeem, S., Fujiki, N., Nevsimalova, S., Uchino, M., Yesavage, J., Di Monte, D., Dohi, K., Melberg, A., Lammers, G.J., et al. (2001). CSF hypocretin/orexin levels in narcolepsy and other neurological conditions. Neurology *57*, 2253–2258.

Sakurai, T., Amemiya, A., Ishii, M., Matsuzaki, I., Chemelli, R.M., Tanaka, H., Williams, S.C., Richardson, J.A., Kozlowski, G.P., Wilson, S., et al. (1998). Orexins and orexin receptors: a family of hypothalamic neuropeptides and G protein-coupled receptors that regulate feeding behavior. Cell *92*, 573–585.

Siegel, J.M. (1979). Behavioral functions of the reticular formation. Brain Res. *180*, 69–105.

Siegel, J.M. (2000). Narcolepsy. Sci. Am. *282*, 76–81.

Siegel, J.M. (2004). Hypocretin (orexin): role in normal behavior and neuropathology. Annu. Rev. Psychol. *55*, 125–148.

Siegel, J.M., and McGinty, D.J. (1978). Pontine reticular formation neurons and motor activity. Science *199*, 207–208.

Siegel, J.M., and Tomaszewski, K.S. (1983). Behavioral organization of reticular formation: Studies in the unrestrained cat. I. Cells related to axial, limb, eye, and other movements. J. Neurophysiol. *50*, 696–716.

Siegel, J.M., Nienhuis, R., Fahringer, H., Paul, R., Shiromani, P., Dement, W.C., Mignot, E., and Chiu, C. (1991). Neuronal activity in narcolepsy: identification of cataplexy-related cells in the medial medulla. Science *252*, 1315–1318.

Sinnamon, H.M., and Polania, L.M. (1997). Coordination of neck and hindlimb extension during the initiation of locomotion elicited by hypothalamic stimulation. Behav. Brain Res. *89*, 289–295.

Soffin, E.M., Evans, M.L., Gill, C.H., Harries, M.H., Benham, C.D., and Davies, C.H. (2002). SB-334867-A antagonizes orexin mediated excitation in the locus coeruleus. Neuropharmacology *42*, 127–133.

Steininger, T.L., Alam, M.N., Gong, H., Szymusiak, R., and McGinty, D. (1999). Sleep-waking discharge of neurons in the posterior lateral hypothalamus of the albino rat. Brain Res. *840*, 138–147.

Thannickal, T.C., Moore, R.Y., Nienhuis, R., Ramanathan, L., Gulyani, S., Aldrich, M., Cornford, M., and Siegel, J.M. (2000). Reduced number of hypocretin neurons in human narcolepsy. Neuron *27*, 469–474.

Thannickal, T.C., Siegel, J.M., and Moore, R.Y. (2003). Pattern of hypocretin (orexin) soma and axon loss, and gliosis, in human narcolepsy. Brain Pathol. *13*, 340–351.

Torterolo, P., Yamuy, J., Sampogna, S., Morales, F.R., and Chase, M.H. (2003). Hypocretinergic neurons are primarily involved in activation of the somatomotor system. Sleep *26*, 25–28.

Torterolo, P., Sampogna, S., Ramos, O., Morales, F.R., and Chase, M.H. (2004). Hypocretinergic system and motor activity in the cat. Sleep Suppl. *27*, A5–A6.

Trulson, M.E., and Jacobs, B.L. (1979). Raphe unit activity in freely moving cats: correlation with level of behavioral arousal. Brain Res. *163*, 135–150.

Valenstein, E.S. (1971). Channeling of responses elicited by hypothalamic stimulation. J. Psychiatr. Res. *8*, 335–344.

Valenstein, E.S., Cox, V.C., and Kakolewski, J.W. (1970). Reexamination of the role of the hypothalamus in motivation. Psychol. Rev. *77*, 16–31.

Vanni-Mercier, G., Sakai, K., and Jouvet, M. (1984). [Specific neurons for wakefulness in the posterior hypothalamus in the cat]. Neurones specifiques de l'eveil dans l'hypothalamus posterieur du chat. C. R. Acad. Sci. III *298*, 195–200.

Vanni-Mercier, G., Gigout, S., Debilly, G., and Lin, J.S. (2003). Waking selective neurons in the posterior hypothalamus and their response to histamine H3-receptor ligands: an electrophysiological study in freely moving cats. Behav. Brain Res. *144*, 227–241.

Veasey, S.C., Fornal, C.A., Metzler, C.W., and Jacobs, B.L. (1997). Single-unit responses of serotonergic dorsal raphe neurons to specific motor challenges in freely moving cats. Neuroscience *79*, 161–169.

Wisor, J.P., Nishino, S., Sora, I., Uhl, G.H., Mignot, E., and Edgar, D.M. (2001). Dopaminergic role in stimulant-induced wakefulness. J. Neurosci. *21*, 1787–1794.

Yamanaka, A., Muraki, Y., Tsujino, N., Goto, K., and Sakurai, T. (2003). Regulation of orexin neurons by the monoaminergic and cholinergic systems. Biochem. Biophys. Res. Commun. *303*, 120–129.

Yoshida, K., McCormack, S., Espana, R., Crocker, A., and Scammell, T. (2004). Afferents to the orexin neurons. Program No. 318.1. Abstract Viewer/Itinerary Planner. (Washington, DC: Society for Neuroscience).